PAPER

Check for updates

Development of an assay for colorimetric and fluorometric detection of H₂S†

Priyotosh Ghosh, Diptiman De and Prithidipa Sahoo (ID) *

Hydrogen sulfide is a highly toxic gas that can produce extremely rapid CNS and respiratory depression and sometimes becomes fatal at high concentrations. There is no proven antidote for hydrogen sulfide poisoning. Hence, it is important to reduce the production of H₂S in several industries, such as oil and gas refining and mining industries. As a consequence, researchers are always inquisitive about inventing different sensing devices or useful tools to detect H₂S selectively in a cost-effective manner. Colorimetric and fluorometric detection methods are the most attractive owing to their simplicity, profitability, ease of understanding, and "on-spot" detection convenience. In this research, we developed some colorimetric and fluorometric chemosensors and established an assay for the easy detection of H₂S following a specific mechanism. The sensing mechanisms were well established through exhaustive spectroscopic studies and theoretical calculations. We first synthesized a series of chemosensors using 2-hydroxy naphthaldehyde as a primary fluorophore. The chemosensors were developed by incorporating various electron-releasing and donating groups while keeping the binding site unchanged. Subsequently, we compared their efficiency and binding ability towards H₂S with a possible mechanism. The chemosensor was employed through a paper strip for demonstration as an "in-field" device by changing the naked-eye and fluorescence color both in liquid and gas phases.

Introduction

Hydrogen sulfide is a recognized toxic gas predominantly emitted from drainage rubbish dumps, stagnant water, laboratory chemical waste, coal mines, and the oil and paper industries.[1–3] The National Institute for Occupational Safety and Health (NIOSH) reports that 100–1000 ppm of H₂S causes serious problems in the respiratory, central nervous, and cardiovascular systems.[4–11] There is no proven antidote for H₂S intoxication and the treatment usually involves support of respiratory and cardiovascular functions. Hence, it needs to be detected before the poison enters and harms the body. As a consequence, it has been prioritized to design and develop diverse sensors for the recognition of H₂S by researchers all over the globe. Visual sensing detection techniques are always fascinating and attractive among all other conventional methods. Compared with the fluorometric method and other methods, the colorimetric method has some noticeable advantages such as cost-effectiveness, user-friendliness, portability, being instrumentation-free, easy-to-regulate properties, real-time detection, and qualitative or semi-qualitative detection *via* the naked eye. Numerous colorimetric and fluorometric

chemosensors have emerged for the detection of hydrogen sulfide through various mechanisms.[12–14] Among these, the deprotonation mechanism stands out owing to its simplicity and easy-to-understand nature for H₂S detection.[15,16]

2-Hydroxy naphthaldehyde is a highly versatile and effective building block for the development of chemosensors aimed at the detection of hydrogen sulfide.[17–20] Its unique structural features and chemical properties make it particularly suitable for the design of sensors that operate *via* deprotonation mechanisms, enabling straightforward and reliable H₂S detection both visually and fluorometrically. H₂S induces the deprotonation of the hydroxyl group, forming a phenolate anion by liberating hydrogen sulfide ions (HS⁻). The formation of the phenolate anion alters the electronic distribution within the naphthalene ring, leading to changes in the absorbance and fluorescence properties of the molecule.

Based on these studies, we have developed a 2-hydroxy naphthaldehyde aminophenol derivative (N1) specifically for H₂S detection, which exhibits a subtle color change from yellow to a deeper yellow in the presence of H₂S. Subsequently, we aimed at synthesizing a series of functionalized probes incorporating various electron-withdrawing (EWG) and electron-releasing groups (ERG) with the same core moiety (2-hydroxy naphthaldehyde) to elucidate the selective efficacy of these probes in detecting H₂S (Table S1†). Initially, we synthesized four distinct derivatives of 2-hydroxy naphthaldehyde to evaluate their sensitivity toward H₂S (Fig. 1). All probes have been

Department of Chemistry, Visva-Bharati University, Santiniketan-731235, India. E-mail: prithidipa.sahoo@visva-bharati.ac.in
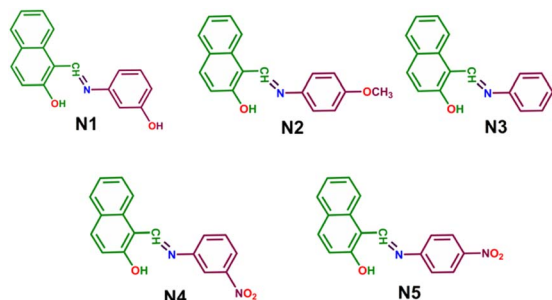
Fig. 1 Synthesis of different derivatives of 2-hydroxy naphthaldehyde.

characterized *via* UV-Vis, fluorescence, NMR and HRMS spectroscopy (Fig. S1–S10†).

Results and discussion

Selectivity

To compare the sensitivity and selectivity of the four derivatives of 2-hydroxy naphthaldehyde towards H_2S, the selectivity experiment was conducted in $DMSO : H_2O$ (1 : 1, v/v) at pH 7.0 (10 mM phosphate buffer). In the naked-eye detection, the addition of H_2S in N5 derivative caused an instant color change from yellow to purple, while the N4 derivative changed the color from yellow to orange within a few seconds (Fig. 2). Likewise, the other two derivatives (N2 and N3) did not exhibit any color change noticeable to the naked eye (Fig. 2F and S11†). We have performed the same experiments with some other relevant anions, which did not show any color change of the probe. This observation demonstrates that the probe having EWG at the *para* position (N5) is very selective and specific for the visual

detection of H_2S. However in the presence of H_2S, N1–N5 don't show any fluorescence spectral change (Fig. S13†).

UV-vis and fluorescence study

The spectral properties of the chemosensors were examined using UV-Vis titration in a $DMSO : H_2O$ (1 : 1) solution using 10 mM phosphate buffer at pH 7.0 (see the pH titration plot, Fig. S13†). The N5 derivative displayed an absorption band at 455 nm (Fig. 2). With the successive addition of H_2S, a new absorption peak appeared at 544 nm, indicating a bathochromic shift of 89 nm. As the concentration of H_2S increased, the absorbance at 544 nm significantly increased, while the band at 455 nm gradually decreased. The presence of a clear isosbestic point at 493 nm suggested a robust interaction between the complex and H_2S. The stoichiometric interaction ratio between the N5 derivative and H_2S is 1 : 1, which is calculated from Job's plot analysis (Fig. S14†). For the derivative N4, the incremental addition of H_2S caused the absorption intensity at 382 nm to gradually decrease, with a new absorption peak appearing at 460 nm. An isosbestic point at 420 nm indicated a strong interaction between the complex and H_2S. The LOD for N5 (65 nM) is much lower than that for N4 (0.72 μM) (Fig. S15 and S16 and Table S2†). The association constant of N5 for H_2S was determined to be 4.15×10^6 M^{-1} (Fig. S17†). In contrast, the N2 and N3 derivatives did not exhibit any significant changes in their absorption spectra or naked eye color changes.

^{1}H NMR titration

To investigate the nature of the binding interaction between the N5 derivative and H_2S, ^{1}H NMR spectra were recorded in DMSO-d_6 and D_2O. Upon interaction with H_2S, the –OH proton at 15.26 ppm and the imine proton at 9.68 ppm disappeared, and two new peaks appeared at 9.46 ppm and 9.20 ppm, indicating the formation of –NH– and =CH– groups. The entire set of aromatic protons shifted upfield, suggesting that the generation of high electron density resulting from the deprotonation
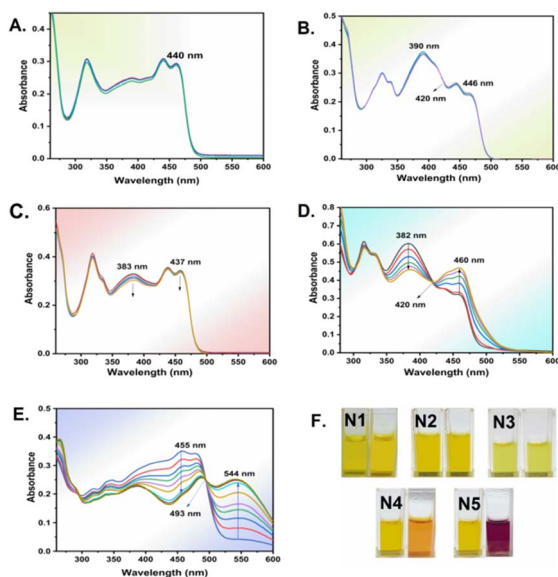

Fig. 2 UV-vis absorption spectra of (A) N1, (B) N2, (C) N3, (D) N4, and (E) N5, (10 μM) upon incremental addition of H_2S (0.9 μM to 7.5 μM) in $DMSO : H_2O$ (1 : 1, v/v) at pH 7.0 (10 mM phosphate buffer). (F) Naked eye color changes in N1, N2, N3, N4, and N5 after the addition of H_2S.
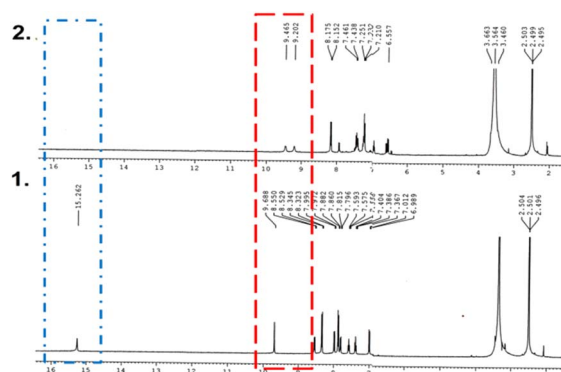

Fig. 3 ^{1}H NMR titration [400 MHz] of the *p*-nitro derivative (N5) in DMSO-d_6 at 25 °C and the corresponding changes after the addition of Na$_2$S in D_2O from (1) only N5 derivative, and (2) N5 derivative + 2 equivalents of Na$_2$S.

of the N5 derivative by H_2S was delocalized throughout the entire molecule (Fig. 3).

Computational studies

Density functional theory (DFT) calculations were performed to optimize the structure of synthesized chemosensors and their complexes using the Gaussian 09 software package. The B3LYP functional and aug ccpvdz basis set were employed for both the ground state and the excited state of the synthesized chemosensors.[21] To incorporate solvent effects, the polarizable continuum model (CPCM) was used. These calculations provided optimized structures of the synthesized chemosensors. For the *p*-nitro derivate (N5), the TDDFT calculation depicts a sharp transition from S_0 to S_1 at 476 nm (oscillator strength, $f = 0.5325$) (Tables S3 and S4†), whereas in complex, the transition from S_0 to S_1 occurs at 500.96 nm (oscillator strength, $f = 0.6576$), corroborating the experimentally observed absorbance at 455 nm and 544 nm, respectively. For the *m*-nitro isomer (N4) the transition from S_0 to S_2 occurs at 388 nm (oscillator strength, $f = 0.5303$), whereas in complex, the transition from S_0 to S_2 occurs at 421 nm (oscillator strength, $f = 0.4923$), which also aligns with the experimental values at 382 nm and 460 nm. The energy difference of the HOMO and LUMO orbital levels for the complex is 0.35 eV, 0.30 eV, and 0.17 eV lower than that of the N3, N4, and N5 derivatives, respectively (Table S5† and Fig. 4).

Plausible mechanism

Based on the experiments and theoretical calculations, it is confirmed that the N5 derivative exhibits greater sensitivity towards H_2S. The proposed sensing mechanism of the chemosensor with H_2S is illustrated in Fig. 5. In the presence of H_2S, the hydroxyl group in the naphthalene moiety of the chemosensor is deprotonated, increasing electron density in the aromatic rings, which results in both color changes and spectral shifts. It is evident that introducing an electron-withdrawing group ($-NO_2$) at the *para* and *meta* positions enhances bathochromic shifts and produces a more intense color change visible to the naked eye. HRMS spectra also corroborated our proposed mechanism (Fig. S18†).
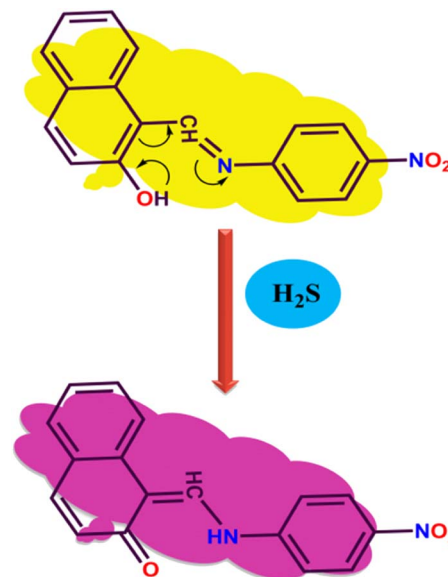

Fig. 5 Sensing mechanism of the N5 derivative for H_2S.

Based on the deprotonation mechanism, we synthesized two 2-hydroxy naphthaldehyde derivatives (N6 and N7) using two different fluorophores keeping the binding site unchanged to investigate any changes in absorbance spectra and visible color along with the fluorescence change (Fig. 6 and S19–S22†).

Upon sequential addition of H_2S, N6 exhibits a visual color change from colorless to deep yellow, attributed to the 1,8-naphthaldehyde moiety acting as a withdrawing group, whereas in the presence of H_2S, N7 shows neither a color change nor a spectral change in UV-vis or fluorescence (Fig. S23†), likely because the carbazole molecule acts as an electron-releasing group (Fig. 7).

Further, we have synthesized another three chemosensors (N8, N9, and N10) without a conjugation between naphthaldehyde and linker molecules to examine any changes in their spectral properties (Fig. 8 and S24–S29†). In the presence of H_2S, N8, N9, and N10 exhibit negligible changes in their absorbance spectra and no color change noticeable to the naked eye (Fig. 9). However, in fluorescence spectra, all three sensors exhibit a significant enhancement in fluorescence intensity.
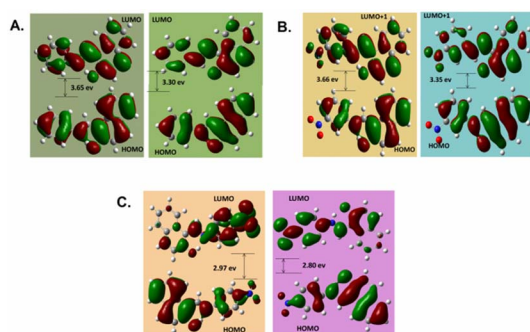

Fig. 4 (A), (B), and (C) are the HOMO and LUMO distributions of N3, N4, and N5 and their complexes with H_2S, respectively.
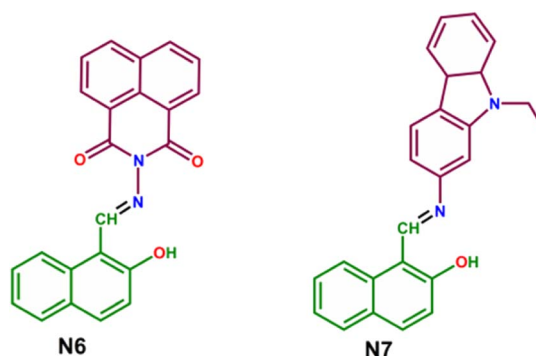

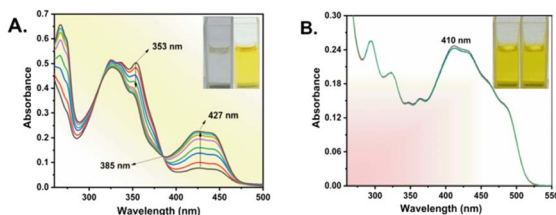**Fig. 6** Other synthesized chemosensors.

Fig. 7   UV-vis absorption spectra of (A) N6 and (B) N7 (10 μM) upon incremental addition of H_2S (0.9 μM to 7.5 μM).
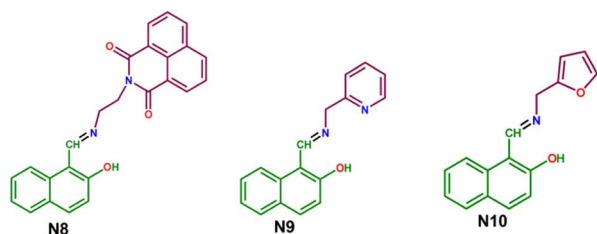

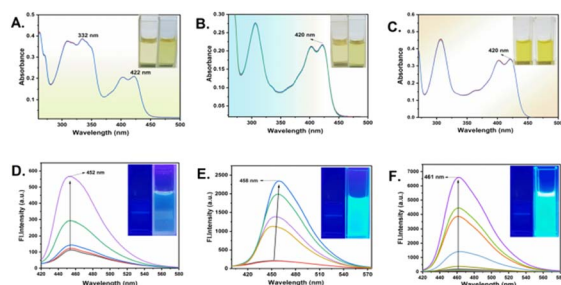Fig. 8   Other synthesized chemosensors (N8, N9, and N10).

Fig. 9   (A), (B) and (C) are the UV-vis absorption spectra of N8, N9, and N10 (10 μM) upon the addition of H_2S up to 1.1 equiv. and (D), (E) and (F) are the emission spectra of N8, N9, and N10 (10 μM) upon incremental addition of H_2S up to 8.9 equiv., 10.2 equiv. and 6.8 equiv., respectively, in DMSO : H_2O (1 : 1, v/v) at pH 7.0 (10 mM phosphate buffer).

With the incremental addition of H_2S, N8 and N9 show emission maxima at 452 nm and 458 nm, with increased fluorescence intensity by about 5-fold and 32-fold, respectively. In contrast, N10 displays an emission maximum at 461 nm with an approximately 100-fold increase in fluorescence. The more electronegative furan facilitates the higher emission maxima of N10 than N9 and hence, attains the rapid deprotonation of the hydroxyl group to produce a vibrant blue fluorescence. In N8, the long ethylene chain between two fluorophores deters the sufficient electron flow that reduces the intensity of fluorescence as shown in Fig. 9.

The significant enhancement in fluorescence is due to the ESIPT "on–off" mechanism through deprotonation of the hydroxyl group in the naphthalene moiety (Fig. 10), which is supported by ^1H NMR titration (Fig. S30†) along with the theoretical studies (Fig. S31†). It was found that N10 has a detection limit of 18 nM for H_2S (Fig. S32†).
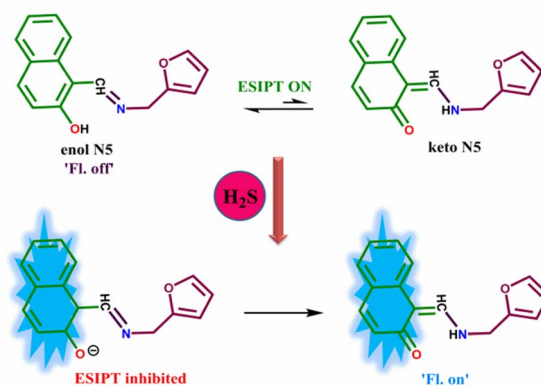

Fig. 10   Sensing mechanism of the N10 derivative for H_2S.

The sensing ability of N5 and N10 towards H_2S has also been successfully demonstrated in both liquid and gas phases, highlighting their potential as a convenient chemosensor kit. Whatman-41 filter paper strips were immersed in N5 and N10 solutions separately.

Upon contact with H_2S, N5 showed a rapid, deep purple color immediately. For N10, a paper strip placed inside a glass chamber containing H_2S gas exhibited a "turn-on" bright blue fluorescence within a few seconds (Fig. 11).

Experimental section

Materials and methods

2-Hydroxy naphthaldehyde, *m*-amino phenol, *p*-nitro aniline, *o*-nitro aniline, aniline, 1,8 naphthalic anhydride, 3-amino-9-ethylcarbazole, picolyl amine, furfuryl amine and sodium sulfide were purchased from Sigma-Aldrich Pvt. Ltd. Unless otherwise mentioned, materials were obtained from commercial suppliers and were used without further purification. Solvents were dried according to standard procedures. Double distilled water was used throughout all experiments. ^1H and ^13C NMR spectra were recorded on a Bruker 400 MHz instrument. For NMR spectra, CDCl_3, DMSO-d_6 and for NMR titration DMSO-d_6 and D_2O were used as solvents using TMS as an internal standard. Chemical shifts are expressed in δ ppm units and ^1H–^1H and ^1H–C coupling constants in Hz. The mass
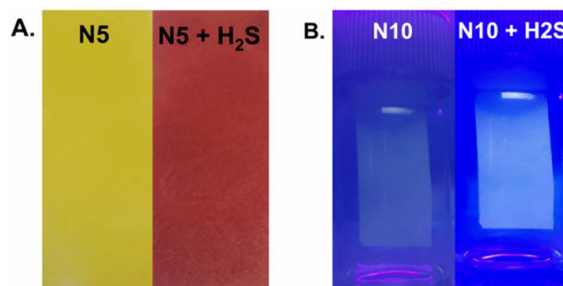

Fig. 11   Display of paper strip sensing of H_2S using (A) an N5-coated filter paper in the absence and presence of H_2S. (B) N10-coated paper strip under a UV lamp in the absence and presence of H_2S.

Scheme 1 Synthetic pathway of 2-hydroxy naphthaldehyde derivatives (N1, N2, N3, N4, and N5).

spectrum (HRMS) was recorded using a Micromass Q-TOF micro™ instrument with methanol as a solvent. Fluorescence spectra were recorded on a Hitachi F-7100 spectrophotometer. UV spectra were recorded on a Hitachi U-2910 spectrophotometer. The following abbreviations are used to describe spin multiplicities in ^{1}H NMR spectra: s = singlet; d = doublet; t = triplet; m = multiplet.

Synthetic procedures

N1, N2, N3, N4, and N5 were synthesized by condensation of 2-hydroxy naphthaldehyde (1 equiv.) and linkers (1.2 equiv.) in MeOH (20 ml) at 70 °C for 12 h (Scheme 1).

Conclusions

In summary, we have synthesized some chemosensors employing 2-hydroxy naphthaldehyde as a key fluorophore, aimed at detecting the toxic hydrogen sulfide (H_2S) through the simple deprotonation mechanism. While developing an assay of chemosensors for the quick detection of H_2S we introduced linkers with various EWGs and EDGs to attach with the main fluorophore and checked their respective colorimetric and fluorometric characteristics with the help of detailed spectroscopic studies and theoretical calculations. The chemosensors containing electron-withdrawing groups displayed a distinct color change visible to the naked eye. In contrast, those with electron-releasing groups showed neither a visual color change nor any spectral variation in the UV-vis spectrum. Furthermore, sensors with disrupted conjugation displayed minimal visible color changes; however, they exhibited a significant "turn-on" bright blue fluorescence through the ESIPT on–off mechanism. With the addition of H_2S, the fluorescence intensity of the probe is enhanced with the cumulative electron-withdrawing nature of the linkers. Moreover, employing a paper strip method, we demonstrated that this approach could be utilized as a practical sensing tool for the real-time detection of H_2S in both liquid and gas phases. This method might be used as a straightforward and efficient means for H_2S detection, enhancing its applicability in various environmental and industrial contexts.

Data availability

The authors confirm that the data supporting the finding of this study are available within the article and its ESI.† Raw data that support the finding of this study are available from the corresponding author upon reasonable request.

Author contributions

PG: writing – original draft, visualization, validation, methodology, investigation, formal analysis, editing; DD: helping with the synthesis of the chemosensors; PS: conceptualization, designing the experiments, funding acquisition, data curation, writing – review & editing, visualization, investigation, and supervision.

Conflicts of interest

There are no conflicts to declare.

Acknowledgements

Notes and references

1 D. K. Aswal and S. K. Gupta, *Science and Technology of Chemiresistor Gas Sensors*, Nova Science Publishers, New York, 2007.
2 A. Mortezaali and R. Moradi, *Sens. Actuators, A*, 2014, **206**, 30–34.
3 S. Maiti, B. Mandal, M. Sharma, S. Mukherjee and A. K. Das, *Chem. Commun.*, 2020, **56**, 9348–9351.
4 A. Papapetropoulos, A. Pyriochou, Z. Altaany, G. Yang, A. Marazioti, Z. Zhou, *et al.*, Hydrogen sulfide is an endogenous stimulator of angiogenesis, *Proc. Natl. Acad. Sci. U. S. A.*, 2009, **106**, 21972–21977.
5 T. S. Bailey and M. D. Pluth, *J. Am. Chem. Soc.*, 2013, **135**, 16697–16704.
6 Q. Wan, Y. Song, Z. Li, X. Gao and H. Ma, *Chem. Commun.*, 2013, **49**, 502–504.
7 K. Abe and H. Kimura, *J. Neurosci.*, 1996, **16**, 1066–1071.
8 H. Kimura, Y. Nagai, K. Umemura and Y. Kimura, *Antioxid. Redox Signaling*, 2005, **7**, 795–803.
9 J. M. Ritter, *Br. J. Clin. Pharmacol.*, 2010, **69**, 573–575.
10 R. Wang, *Physiol. Rev.*, 2012, **92**, 791–896.
11 R. Wang, *Antioxid. Redox Signaling*, 2003, **5**, 493–501.
12 S. Kundu and P. Sahoo, *New J. Chem.*, 2019, **43**, 12369.
13 S. Das and P. Sahoo, *Sens. Actuators, B*, 2019, **291**, 287–292.
14 A. Ghosh, *et al.*, *ACS Omega*, 2018, **3**, 11617–11623.
15 D. A. Thai and N. Y. Lee, *Anal. Methods*, 2021, **13**, 1332.
16 A. K. Manna, J. Mondal, R. Chandra, K. Rout and G. K. Patra, *Anal. Methods*, 2018, **10**, 2317–2326.
17 A. K. Das and S. Goswami, *Sens. Actuators, B*, 2017, **245**, 1062–1125.
18 A. Roy, S. Dey, S. Halder and P. Roy, *J. Lumin.*, 2017, **192**, 504–512.
19 A. Sahana, *et al.*, *Org. Biomol. Chem.*, 2011, **9**, 5523–5529.
20 P. Chowdhury, S. Panja and S. Chakravorti, *J. Phys. Chem. A*, 2003, **107**(1), 83–90.

21 M. J. Frisch, G. W. Trucks, H. B. Schlegel, G. E. Scuseria, M. A. Robb, J. R. Cheeseman, G. Scalmani, V. Barone, B. Mennucci, G. A. Petersson, H. Nakatsuji, M. Caricato, X. Li, H. P. Hratchian, A. F. Izmaylov, J. Bloino, G. Zheng, J. L. Sonnenberg, M. Hada, M. Ehara, K. Toyota, R. Fukuda, J. Hasegawa, M. Ishida, T. Nakajima, Y. Honda, O. Kitao, H. Nakai, T. Vreven Jr, J. A. Montgomery, J. E. Peralta, F. Ogliaro, M. Bearpark, J. J. Heyd, E. Brothers, K. N. Kudin, V. N. Staroverov, R. Kobayashi, J. Normand, K. Raghavachari, A. Rendell, J. C. Burant, S. S. Iyengar, J. Tomasi, M. Cossi, N. Rega, J. M. Millam, M. Klene, J. E. Knox, J. B. Cross, V. Bakken, C. Adamo, J. Jaramillo, R. Gomperts, R. E. Stratmann, O. Yazyev, A. J. Austin, R. Cammi, C. Pomelli, J. W. Ochterski, R. L. Martin, K. Morokuma, V. G. Zakrzewski, G. A. Voth, P. Salvador, J. J. Dannenberg, S. Dapprich, A. D. Daniels, O. Farkas, J. B. Foresman, J. V. Ortiz, J. Cioslowski and D. J. Fox, *Gaussian 09, Revision A. 02*, Gaussian, Inc., Wallingford CT, 2009.